Combustion and Flame 163 (2016) 31–41

Contents lists available at ScienceDirect

Combustion and Flame

journal homepage: www.elsevier.com/locate/combustflame

Pyrolysis and ignition of a polymer by transient irradiation

Izabella Vermesi [a], Nils Roenner [a], Paolo Pironi [b], Rory M. Hadden [b], Guillermo Rein [a,*]

[a] Imperial College London, Department of Mechanical Engineering, London SW7 2AZ, United Kingdom
[b] BRE Centre for Fire Safety Engineering, University of Edinburgh, Edinburgh EH9 3JL, United Kingdom

ARTICLE INFO

Article history:
Received 31 January 2015
Revised 4 August 2015
Accepted 12 August 2015
Available online 5 November 2015

Keywords:
Pyrolysis
Radiation
Heat transfer
Polymethyl methacrylate

ABSTRACT

Pyrolysis is the thermochemical process that leads to the ignition of a solid fuel and a key mechanism in flame spread and fire growth. Because polymeric materials are flammable and ubiquitous in the modern environment, the understanding of polymer pyrolysis is thus essential to tackle accidental fires. In this paper, we used transient irradiation as an external source of heat to study the process of pyrolysis and ignition of a polymer. While previous ignition studies use constant irradiation, transient irradiation is the most frequent condition found in accidental fires, but it lacks a theoretical framework since it has been ignored in the literature. Moreover, transient irradiation is a more comprehensive case for the understanding of pyrolysis where nonlinear heat transfer effects challenge the validity of solid-phase criteria for piloted ignition developed previously. We propose here that transient irradiation is the general problem to solid fuel ignition of which constant irradiation is a particular case. In order to investigate how this novel heat source influences polymer pyrolysis and flammability, numerical simulations and experiments have been conducted on poly(methyl methacrylate) (PMMA) samples 100 mm by 100 mm and 30 mm deep exposed to a range of parabolic pulses of irradiation. The 1D model, coded in GPyro, uses heat and mass transfer and single-step heterogeneous chemistry, with temperature dependent properties. The predictions are compared to experiments conducted in the cone calorimeter for the constant irradiation and the Fire Propagation Apparatus for transient irradiation. The experiments validate the temperature predictions of the model and also provide the time to ignition. The model then complements the experiments by calculating the mass loss rate. A series of 16 parabolic pulses (including repeats) are investigated with a range of peak irradiation from 25 to 45 kW/m^2, while the time to peak ranges from 280 to 480 s. For these pulses, the time to ignition measurements range from 300 to 483 s. The model can predict the in-depth temperature profiles with an average error lower than 9%. Model and experiments are then combined to study the validity of the solid-phase criteria for flaming ignition found in the literature, namely critical temperature, critical mass loss rate, critical energy and critical time-energy squared. We find that of these criteria, the best predictions are provided by the critical mass loss rate followed by the critical temperature, and the worst is the critical energy. Further analysis reveals the novel concept of simultaneous threshold values. While the mass loss rate is below 3 g/m^2 and the surface temperature is below 305 °C, ignition does not occur. Therefore these threshold values when exceeded simultaneously establish the earliest time possible for ignition.

1. Introduction

Fire is a complex phenomenon that encompasses a series of chemical and physical processes [1]. Before the combustible material can undergo combustion and release heat, it has to undergo ignition, which is a critical process that determines the initial growth of the fire [2]. Ignition is the onset of combustion, and flaming ignition the process by which the fast, exothermic, homogenous reaction is started, which then spreads further in the material, causing mass burning [3].

However, before flaming can occur, the solid fuel has to become gaseous [2–4]. The process through which the solid undergoes chemical decomposition and simultaneously transforms into gaseous fuel is called pyrolysis [3,4]. Because the molecules of solid hydrocarbon fuels like synthetic polymers or wood are large, they cannot be oxidized directly. Therefore, when exposed to heat, these molecules irreversibly decompose into smaller hydrocarbon chains which emerge as pyrolyzate gas [5]. Under the right conditions, these can ignite above the surface of the solid. Pyrolysis is the key process in the burning of solid fuels, because the rate at which a material transforms

* Corresponding author.
E-mail address: grein@imperial.ac.uk, g.rein@imperial.ac.uk, reingu@gmail.com (G. Rein).

http://dx.doi.org/10.1016/j.combustflame.2015.08.006

Nomenclature

Symbol	Description
A	pre-exponential factor
C	proportionality factor between time and energy-squared
c_p	heat capacity
E	activation energy
ΔH	heat of reaction
h_c	convective heat transfer coefficient
k	thermal conductivity
L	depth of the sample
$\dot{m}''$	mass flux per unit area
m''	mass per unit area
Q	energy
$\dot{q}''$	heat flux
$\dot{Q}'''$	heat generation per unit volume
R	universal gas constant
T	temperature
t	time
Y	mass fraction
z	depth into the sample

Greek letters

Symbol	Description
ε	emissivity
κ	radiative absorption coefficient
$\dot{\omega}'''$	reaction rate per unit volume
ρ	density
σ	Stefan–Boltzmann constant

Subscripts

Symbol	Description
0	initial
Al	aluminium
e	external
d	destruction
g	gas
i	condensed-phase species index
ig	at ignition
p	at peak
r	in-depth radiation
s	solid

into a gas phase fuel governs the timing of ignition and the energy release rate in the subsequent flames [4].

Most ignition studies consider constant irradiation representing the radiant irradiation from the heat source [3]. The exception to the ignition studies is the work by Reszka et al. [6] which considers a linearly increasing irradiation on a series of fuel types, and the work by Belcher et al. [7] which uses parabolic heat pulses. While using a constant irradiation is convenient due to its simplicity, this scenario is not realistic. Moreover, transient irradiation is a more comprehensive case for the understanding of pyrolysis where nonlinear heat transfer effects challenge the validity of solid-phase criteria for flaming ignition developed previously. We propose here that transient irradiation is the general problem to solid fuel ignition of which constant irradiation is a particular solution. It is essential to understand how and when ignition is reached with both constant and transient irradiation. This paper aims to carry out that study by combining numerical and experimental work. A parabolic pulse is chosen here because it is the simplest curve including both growth and decay.

The investigation of the ignition is done by comparing complementary experimental and computational works that use transient irradiation to investigate the pyrolysis of poly(methyl methacrylate) (PMMA), a polymer widely studied in fire science. The experiments measured the temperature profiles in PMMA samples heated by different irradiation pulses, thus providing validation for the numerical model.

This paper begins by summarizing the theoretical background on the classical ignition theory and four different ignition criteria found in the literature: critical energy, critical temperature, critical mass flux and time-energy squared. Afterwards, the experimental work is presented. The computational work, performed in a 1D pyrolysis model, GPyro [8], is then presented and validated using benchmark experiments by Kashiwagi et al. [9]. The results of the simulations are then compared to the transient irradiation experiments. Finally, the ignition criteria are assessed with respect to both constant and transient irradiation.

2. Classical ignition

Pyrolysis occurs inside the solid phase, and produces the gases necessary to feed the flame. In order to study flame ignition with a focus on solid-phase phenomena, there is need to replace the gas phase and invoke an ignition criterion. This criterion describes when ignition of the gas phase would take place by referring to conditions in the solid phase alone. In the literature, there are four criteria for piloted ignition. All four are empirical but based on combustion theories of different degrees of development. These are the critical energy, critical temperature, critical mass flux and time-energy squared.

For a thermally thick solid, the critical temperature criterion leads to Eq. (1) to establish the time to ignition calculated from the assumption of a critical surface temperature and a constant irradiation [4]. It is the most commonly used ignition criterion. It takes into account two main parameters, namely the ignition temperature and the thermal inertia of the fuel. However, this approach has several limitations. The greatest limitation is the difficulty of measuring the critical temperature [5], and its variation with regards to external heat flux and environmental conditions such as oxygen concentration. Therefore, the critical temperature criterion cannot give a certain value applicable for each fuel, but it varies with conditions under which it was determined [4,10].

$$\frac{1}{\sqrt{t_{ig}}} = \frac{2}{\sqrt{\pi}\sqrt{k\rho c}} \frac{\dot{q}_e''}{T_{ig} - T_0} \tag{1}$$

The critical mass loss rate is considered the most fundamental criterion. It assumes that ignition takes place when a critical flow of pyrolyzate mixes with air such that the mixture surpasses the lower flammability limit at the location of the pilot [3]. However, the experimental measurements are quite difficult, because the mass loss rate before ignition is very low [5]. Rich et al. [11] have proposed a theoretical model that relates the critical mass flux necessary for ignition to fuel properties using Spalding's number [12] and to environmental characteristics [11].

The critical energy criterion states that a sample will ignite after absorbing a certain amount of energy. The energy criterion relies on a series of simplifications, such as negligible heat losses and a constant ignition temperature [5]. Therefore, the criterion provides ranges of critical energy rather than a single value for each material.

$$Q_{ig} = \int_0^{t_{ig}} \dot{q}_e'' dt \tag{2}$$

The only criterion in the literature developed for transient irradiation is the time-energy squared correlation. This has been developed by Reszka et al. [6] and calculates the time to ignition by finding the squared integral of the incident irradiation up to the elapsed time. This method is applicable for incident irradiation fluxes that grow linearly. The methodology for this criterion relies on the linear dependency between $t_{ig}^{-\frac{1}{2}}$ and $\dot{q}_{ext}''$ and results in Eq. (3), where C represents

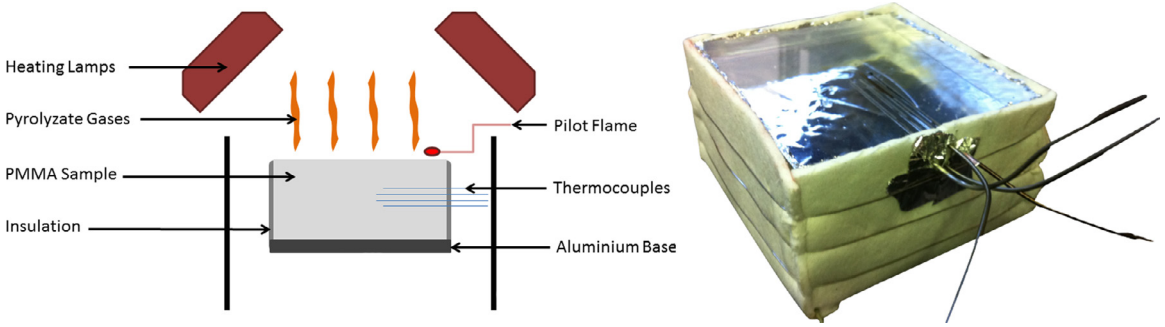

Fig. 1. Sketch of the test setup (left) and a prepared PMMA sample (right).

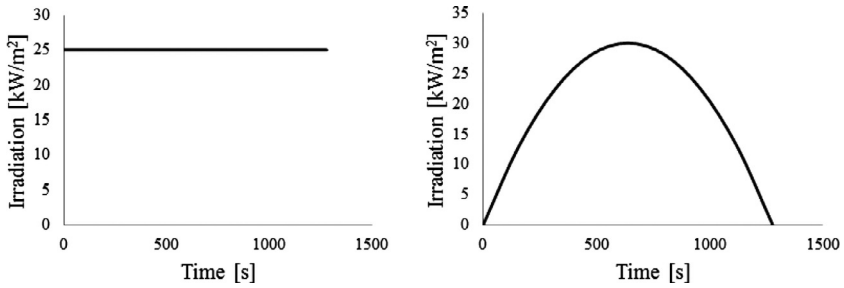

Fig. 2. Constant irradiation (left), which is used in most literature and the parabolic irradiation pulse (right), applied in this paper.

Table 1
Typical ignition criteria values for PMMA found in literature.

Ignition criteria	Value of parameter
Critical energy	2 MJ/m^2 (irradiance of 30 kW/m^2) [5]
Critical mass flux	2.0 g/m^2 s [13], 1.9–3.2 g/m^2 s [14]
Critical temperature	250–400 °C [15], 380 °C [4]
Critical time-energy squared	226 GJ^2/m^4 s [6]

Table 2
List of experiments using parabolic irradiation pulses.

Experiment no.	Peak irradiation (kW/m^2)	Time to peak (s)	Irradiation pulse duration (s)
1, 2, 3	30	320	640
4, 5, 6	45	320	640
7, 8, 9	25	320	640
10, 11, 12, 13	30	480	960
14, 15, 16	30	260	520

the linearity coefficient and it depends on the irradiation scenario, having different values for constant irradiation, for linear irradiation and for parabolic pulses.

$$Q_{ig}^2/t_{ig} = C \tag{3}$$

The four ignition criteria are applied to PMMA with values taken from the literature. PMMA, commonly called plexiglass, is one of the most common polymers studied in fire science, therefore there is substantial experimental and computational data available for comparison. It is a non-charring thermoplastic polymer that has different grades and blends. A commercial cast grade PMMA is used for the experiments in this study. The ranges found in the literature for the critical parameters are presented in Table 1.

3. Experiments

Experiments were conducted in a Fire Propagation Apparatus (FPA) using a set-up based on the standard piloted ignition test described in ASTM E2058 [16]. A specimen of the sample material was subjected to irradiation on its upper surface from an external radiant source and a pilot flame. The irradiation was provided by four infrared heaters each containing six tungsten filament tubular quartz lamps. Parabolic irradiation-time pulses with different duration and maximum irradiation were used for each group of experiments, as shown in Table 2 and Fig. 2. In-depth temperature profile was measured with four type-K thermocouples inserted parallel to the heated surface at depths of 2, 5, 8 and 10 mm, as illustrated in Fig. 1. The thermocouples were sheathed, thus having no exposed beads, and had a uniform diameter of 1.5 mm along their length. This methodology has been used previously in [17,18] and yielded good results, with a maximum error of 10%. Because the transient heating of the material is slow, issues related to thermocouple diameter, such as lag, are negligible. In order to characterize the heat transfer at the bottom boundary of the sample, the set-up incorporated a large aluminium block at the bottom face. The temperature of the block was measured by a thermocouple inserted in the centre [18].

Commercial sheets of PMMA were pre-cut into 100 mm × 100 mm × 30 mm samples. Prior to testing, the base of the sample and its sides were wrapped in a layer of aluminium foil. The sample and aluminium block were then tightly wrapped in a layer of ceramic paper for thermal insulation, secured by 3 pieces of thin wire wrapped around the outside. The irradiation-time pulses were generated by sampling the target parabolic curves at 10 s intervals and varying the voltage applied to the lamps according to calibration. The pilot flame was ignited prior to the beginning of the test and maintained on throughout the experiment, as shown in Fig. 1.

An example of temperature histories for the 30 kW/m^2 experiments with in-depth temperature measurements are presented in Fig. 3. The parabolic irradiation is represented in Fig. 2. The repeatability of the time-temperature pulses and the ignition delay time is very high. The sample did not ignite when subjected to a shorter pulse duration (520 s) peaking at 30 kW/m^2, or to a lower peak (25 kW/m^2).

Mass loss measurements in transient irradiation are challenging due to the excessive noise due to unsteady buoyancy and the small signal at ignition. But mass loss rate is important to understand ignition, so in this paper we predict it numerically and no weight measurements are made.

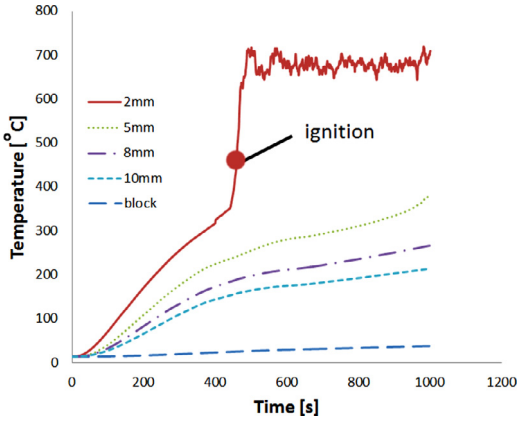

Fig. 3. Average temperature-time curves for experiments 1 and 2: transient irradiation peaking at 30 kW/m^2 after 320 s. Legend shows measurements at different depths from the free surface.

To investigate a wider applicability of the results beyond the transient irradiation with the tungsten lamps of the FPA, additional data is collected under constant irradiation in a cone heater. For these tests, the samples, prepared in an identical manner as described, are placed in a calibrated cone heater under 15 kW/m^2 and 20 kW/m^2 irradiation.

4. Numerical model

4.1. Gpyro

The one-dimensional (1D) numerical model for this study was developed in GPyro, an open-source software that represents the state of the art in pyrolysis modelling [8]. The 1D assumption is valid for this case because the characteristic length is much larger than the thickness of the sample. The governing equations for the solid (condensed) phase are detailed in Eq. 4 for the mass, Eq. (5) for the species, and Eq. (6) for the energy. For more details, refer to [19].

$$\frac{\partial \bar{\rho}}{\partial t} = -\dot{\omega}_g''' \tag{4}$$

$$\frac{\partial (\bar{\rho} Y_i)}{\partial t} = -\dot{\omega}_{di}''' \tag{5}$$

$$\frac{\partial (\bar{\rho}\bar{h})}{\partial t} = \frac{\partial}{\partial z}\left(\bar{k}\frac{\partial T}{\partial z}\right) + (-\dot{\omega}_{di}''')\Delta H_s - \frac{\partial \dot{q}_r''}{\partial z} \tag{6}$$

The state of the art chemistry for PMMA pyrolysis is a three step process [10]. However, Bal and Rein [20] have shown that the heat transfer in the solid phase is dominant and the chemistry is of secondary importance in defining the pyrolysis. Therefore, a one-step reaction scheme is used as the uncertainty associated with a more complex kinetic scheme outweighs the improvements in accuracy (as confirmed in later sections).

The pyrolysis rate of the sample is calculated by a temperate-dependent Arrhenius term presented in Eq. (7).

$$\dot{\omega}_i = \frac{\partial m_i''}{\partial t} = m_{i0}'' A_i e^{-E_i/RT}\left(\frac{m_i''}{m_{i0}''}\right)^{n_i} \tag{7}$$

The domain used in the simulations represents the experimental set-up, as shown in Fig. 4. The equation for the bottom boundary (adiabatic) is shown in Eq. (8), where $z = L$. The sample is a two-layer system and zero contact thermal resistance is assumed between the PMMA and the aluminium. The generalized boundary condition including emissive, convective and irradiative terms, is shown in

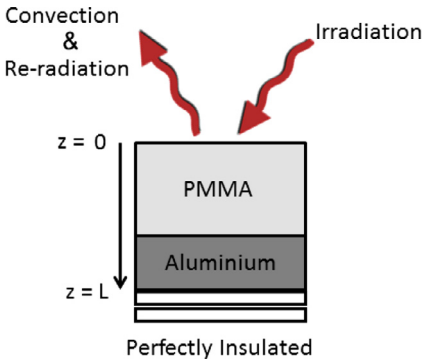

Fig. 4. The computational domain and the boundary conditions.

Eq. (9) and is applied at the top surface, where $z = 0$. The in-depth absorptivity is accounted for using Eq. (10) [8]. While in-depth absorption of external radiation is important in a important translucent fuel [10,21], the in-depth emission is not because the range of values of in-depth temperature below away from the free surface is low. Therefore, the in-depth emission across a PMMA sample can be accurately modelled by a surface emission of 0.95 [10].

$$-\bar{k}\frac{\partial T(L)}{\partial z} = 0 \tag{8}$$

$$-\bar{k}\frac{\partial T(0)}{\partial z} = \bar{\varepsilon}\dot{q}_e'' - h_c(T_s - T_0) - \bar{\varepsilon}\sigma(T^4 - T_0^4) \tag{9}$$

$$-\frac{\partial \dot{q}_r''}{\partial z} = \bar{\varepsilon}\dot{q}_e''\bar{\kappa}e^{-\bar{\kappa}z} \tag{10}$$

The effect of the time and space discretization of the equations on the results is investigated by a sensitivity analysis performed using a simulation with 25 kW/m^2 which peaks at 320 s. The results are shown in Fig. 5. Keeping a balance between accuracy and simulation time, the final values of the domain parameters are chosen: a size of 0.05 mm and a time step of 0.05 s.

4.2. Model validation against benchmark

To verify the simplifications adopted, the work of Kashiwagi et al. [9] is taken as reference. The experiments were pioneering in this field and the results represent high fidelity data. Constant irradiation of a PMMA sample was studied under varying atmospheric conditions, with the temperature at surface and the mass loss measured. The experiments were conducted for 40 kW/m^2 and 17 kW/m^2 fluxes.

These experiments were simulated by Lautenberger et al. in [22] with a chemical scheme of three steps. Using this basis, the effects of the simplifications can be studied in detail and compared to well established data.

As a first step the original Lautenberger model is replicated and then the simplifications of the reduced 1-step chemistry applied. The comparison for the 40 kW/m^2 experiment [9] is shown in Fig. 6. It can be seen that despite the reduction in complexity most of the accuracy of the simulation is retained. However, because these experiments are the only mass loss rate measurements that can be used for comparison with the model, it is important to note that there is a maximum error of 25% induced by the modelling assumptions. This is considered acceptable for the simulation purposes and the progression to the single-step chemistry model is made.

4.3. Parametric study

Due to the transient nature of the scenario, most properties are considered temperature dependent (as opposed as to the common

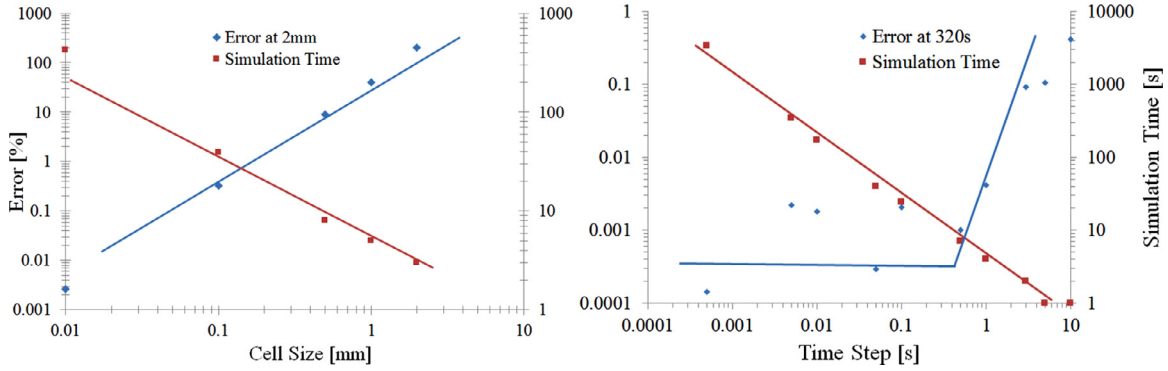

Fig. 5. Error sensitivity with respect to grid size (left) and time step (right).

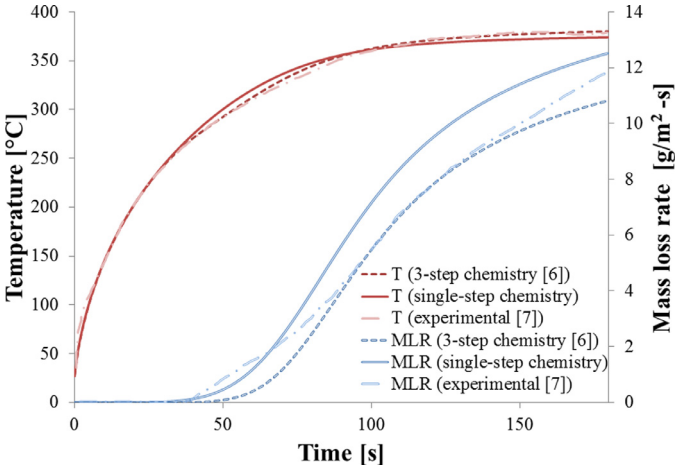

Fig. 6. Validation of single-step chemistry model against Lautenberger's three-step chemistry [8] and Kashiwagi's experimental results [9]: surface temperature results for a sample exposed to constant heat flux of 40 kW/m^2 on the left and mass loss rate results on the right.

assumption of constant effective properties, see [10] for details). Our justification is two-fold. First, there are large differences in property values of PMMA across the temperature range observed in the experiments (from 30 to 700 °C). Moreover, in transient irradiation, there is first heating and then cooling regimes, which challenges the concept of a constant effective value. This alternation is not present in constant irradiation conditions and would substantivally affect the value of any overall effective parameter. These properties are assessed using Eq. (11), shown here for thermal conductivity. The reference temperature T_{ref} is taken as 300 K.

$$k(t) = k_0\left(\frac{T}{T_{\text{ref}}}\right)^{n_k} \tag{11}$$

Because the material properties of PMMA as reported in the literature vary significantly, a parameter sensitivity analysis was performed to see how the temperature and mass loss respond to the change in parameters. Typical ranges for PMMA are extracted from the review by Bal [15] and the maxima and minima are compared to a base case in terms of temperature response near the surface (2 mm) and in-depth (10 mm), as well as the mass loss response. The analysis is presented in Figs. 7 and 8. These figures show the most important material properties of the PMMA in order to obtain reliable results. Some parameters, like emissivity, influence the results mostly at the surface, whereas others, such as the in-depth absorption, are influential in-depth.

Specific heat capacity is the parameter inducing the largest variation, both at surface level and in-depth. The one that induces the least variation is the compensation effect of kinetics, which couples the parameters of pre-exponential factors and activation energy.

Table 3
Baseline modelling parameters: temperature dependent properties for PMMA [22].

Temperature dependent parameters Property	Value	Exponent value	Units
Thermal conductivity k	0.2	−0.19	W/mK
Density ρ	1190	−0.12	kg/m^3
Specific heat capacity c_p	1606	0.89	J/kg K

Table 4
Baseline modelling parameters: in-depth absorptivity κ [21].

In depth absorptivity κ Heat source	Value	Units
Tungsten lamp	225	m^{-1}
Cone	1000	m^{-1}

Table 5
Baseline modelling parameters: properties of aluminium block [23].

Properties of aluminium Property	Value	Units
Thermal conductivity k_{Al}	244	W/mK
Density ρ_{Al}	2700	kg/m^3
Specific heat capacity $c_{p,\text{Al}}$	921	J/kg K
Emissivity of aluminium ϵ	1	–

Table 6
Baseline values for kinetic constants [9].

Kinetic constants Property	Value	Units
Pre-exponential factor A	200	s^{-1} × 10^6
Activation energy E	125	kJ/mol
Heat of reaction ΔH_s	540	kJ/kg
Reaction order n	1	–

The model parameters for the base case are listed in Table 3 for the temperature dependent properties, Table 4 for the in-depth absorptivity, Table 5 for the properties of the aluminium block, Table 6 for the kinetics constants and Table 7 for other important parameters. To justify the chosen values for emissivity and in-depth absorptivity, in Bal et al. [10] it is shown that an emissivity value of 0.95, and our equations for the in-depth absorption can reproduce in detail and with a very low error the in-depth temperature profile of PMMA for a wide range of constant irradiation levels.

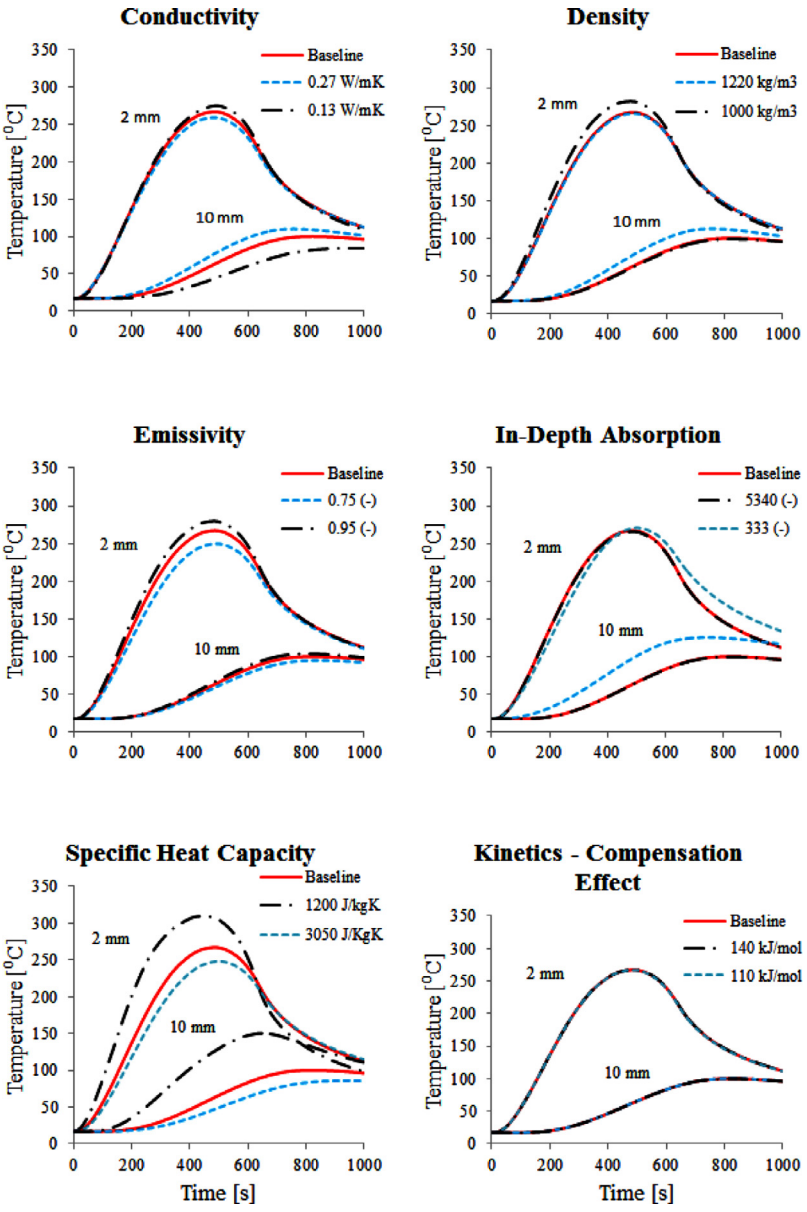

Fig. 7. Sensitivity of the predicted surface temperatures to varying material properties. Predictions at two depths into the sample are reported: 2 mm and 10 mm from the surface.

Table 7
Miscellaneous properties.

Miscellaneous properties Property	Value	Units
Convective heat transfer coefficient h_c	10	W/m^{2}K
Gas phase specific heat capacity c_p	1003	kJ/kg K
Ambient temperature T	20	°C
Surface emissivity of PMMA ϵ [10]	0.95	

5. Transient irradiation results

The first experiments studied numerically are those of constant irradiation, because it is the most common test condition in the literature and the simplest irradiation condition. Therefore, obtaining good results in a constant irradiation case is a prerequisite to model more comprehensive conditions. The two cases presented in Figs. 9 and 10 replicate the two constant irradiation test case done in the complementary experiments. The simulations run up to 520 s, when ignition was observed in the case of the 20 kW/m^2 irradiation and when the thermocouples became exposed due to the sample mass lost in the 15 kW/m^2 case, which did not ignite. The experiments were perfomed only once. The temperature results show excellent agreement, with an average error of 3.2%.

For the transient irradiation, all the experiments are predicted numerically in Figs. 11–15. The temperature and mass loss response are shown in comparison with the experimental results. They capture the peak irradiation, as well as the time to peak, marking the first time that a transient irradiation model is used to predict the pyrolysis of PMMA. The errors are in the range of 10% for all the cases, with a large contribution to this error being brought by temperature predictions at the aluminium block. By predicting the mass loss rate, this model also complements the experimental work and allows for the reevaluation of the critical mass loss rate criterion found experimentally.

The ignition results and the irradiation pulses are summarized in Fig. 16. The cases that did not ignite, namely the reduced time to peak and the reduced peak irradiation, are in dashed line and the entire irradiation pulse is shown. In the remaining cases, the ones where

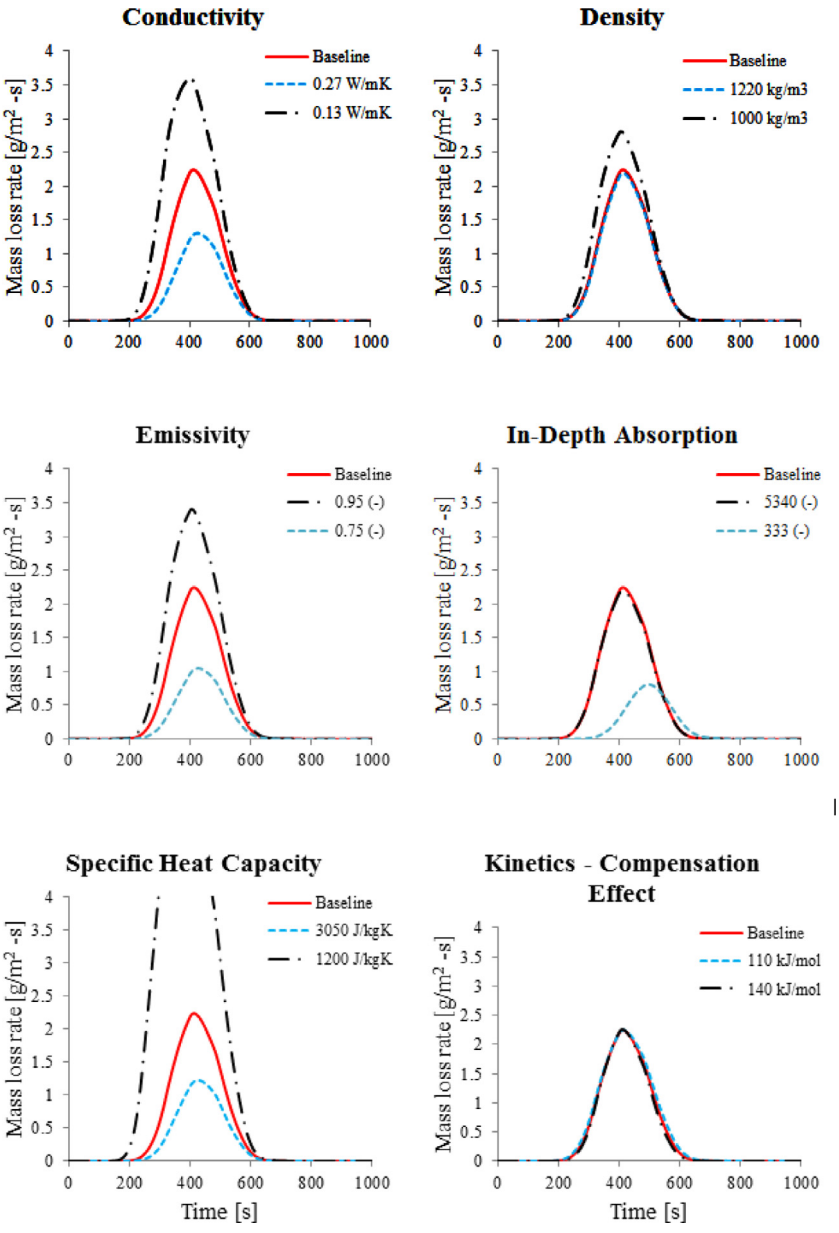

Fig. 8. Sensitivity of the predicted mass loss rate to varying material properties.

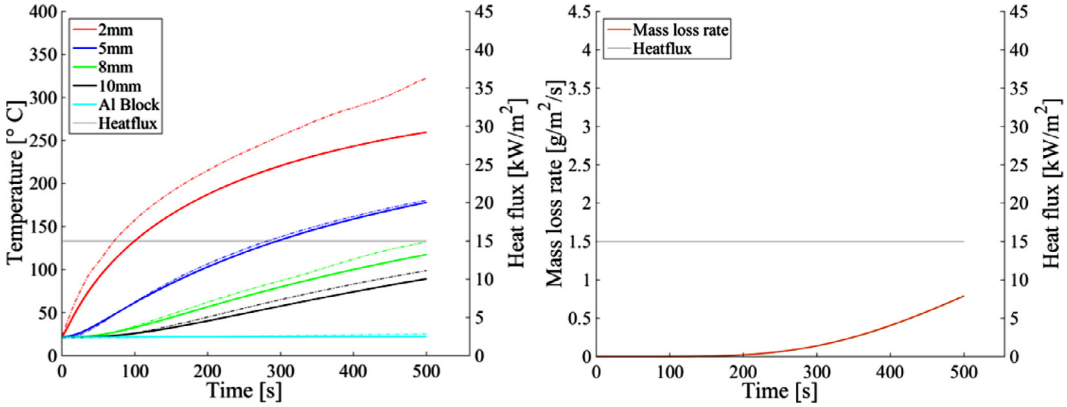

Fig. 9. Constant irradiation of 15 kW/m^2: temperature (a) and predicted mass loss rate (b) at different depths of a PMMA sample; predictions shown in solid, experiments with dashed line (experiments conducted in cone calorimeter).

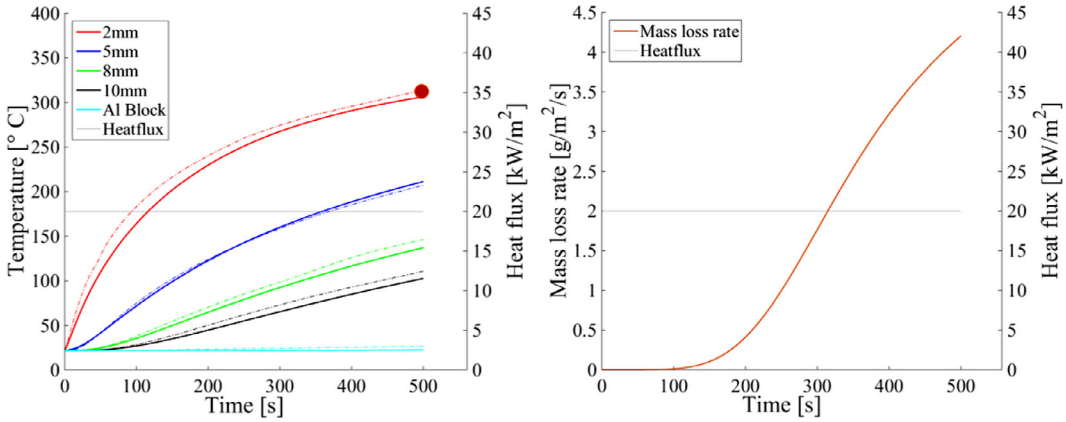

Fig. 10. Constant irradiation of 20 kW/m^2: temperature (a) and predicted mass loss rate (b) at different depths of a PMMA sample; predictions shown in solid, experiments with dashed line (experiments conducted in cone calorimeter).

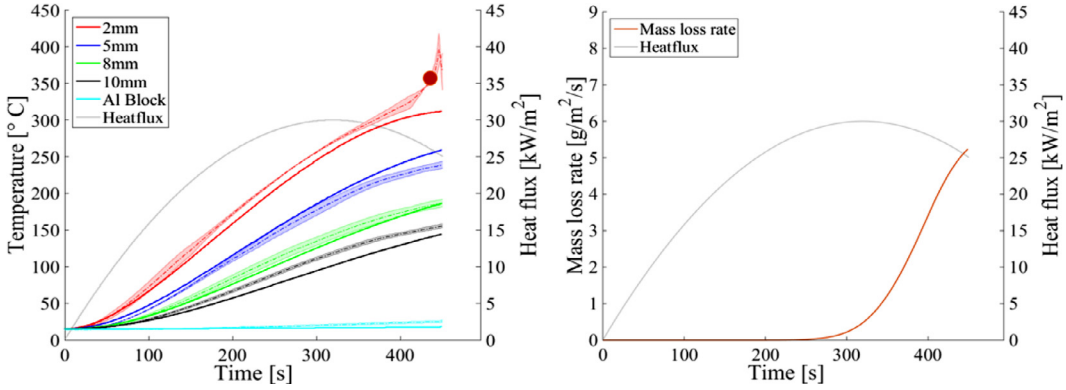

Fig. 11. Transient irradiation peaking at 30 kW/m^2 after 320 s: temperature (a) and predicted mass loss (b) response at different depths of a PMMA sample; predictions shown in solid, experiments with dashed line; error ranges are shown as clouds (sometimes too thin to see); ignition marked with red dot. (For interpretation of the references to colour in this figure legend, the reader is referred to the web version of this article.)

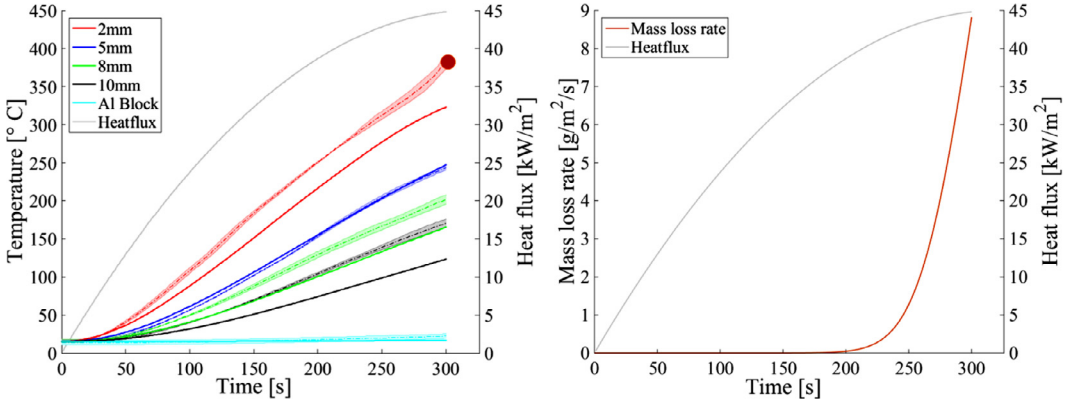

Fig. 12. Transient irradiation peaking at 45 kW/m^2 after 320 s: temperature(a) and predicted mass loss (b) response at different depths of a PMMA sample; predictions shown in solid, experiments with dashed line; error ranges are shown as clouds (sometimes too thin to see); ignition marked with red dot. (For interpretation of the references to colour in this figure legend, the reader is referred to the web version of this article.)

ignition occurred, the irradiation pulse is shown until the ignition time.

5.1. Ignition criteria

This section analyses how the different ignition criteria fare in constant and transient irradiation conditions. The four criteria presented previously in Section 2 are implemented such that their validity is investigated using all the experimental and numerical data available in the study. Table 8 summarizes these results and compares them to values from literature.

The critical energy criterion has similar values for all the experiments, regardless whether ignition occurred or not. This lack of resolution makes it impossible to establish a critical value for ignition.

The criterion which uses the time-energy squared correlation proves to have limited applicability. As shown in [6], there is a

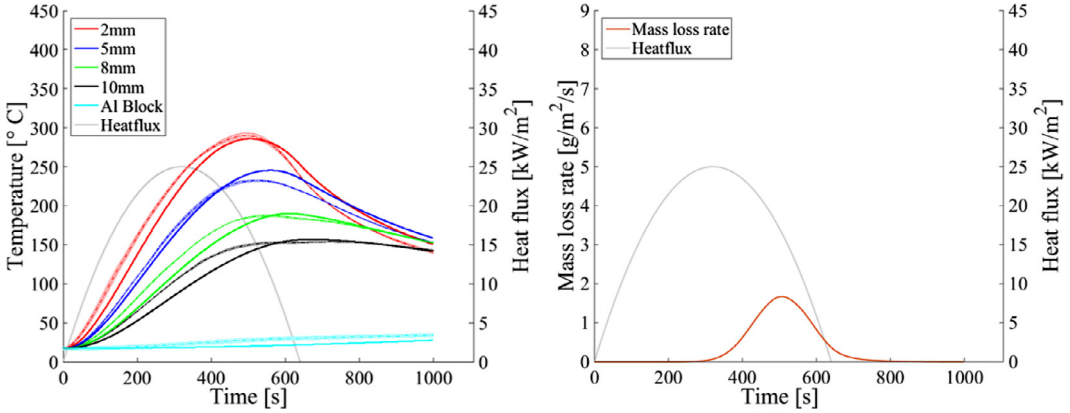

Fig. 13. Transient irradiation peaking at 25 kW/m^2 after 320 s: temperature (a) and predicted mass loss (b) response at different depths of a PMMA sample; predictions shown in solid, experiments with dashed line; error ranges are shown as clouds (sometimes too thin to see).

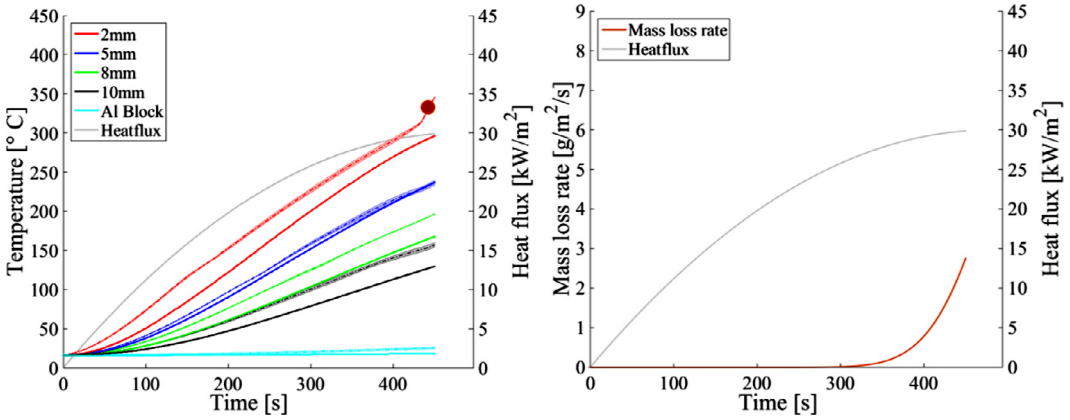

Fig. 14. Transient irradiation peaking at 30 kW/m^2 after 480 s: temperature (a) and predicted mass loss (b) response at different depths of a PMMA sample; predictions shown in solid, experiments with dashed line; error ranges are shown as clouds (sometimes too thin to see); ignition marked with a red dot. (For interpretation of the references to colour in this figure legend, the reader is referred to the web version of this article.)

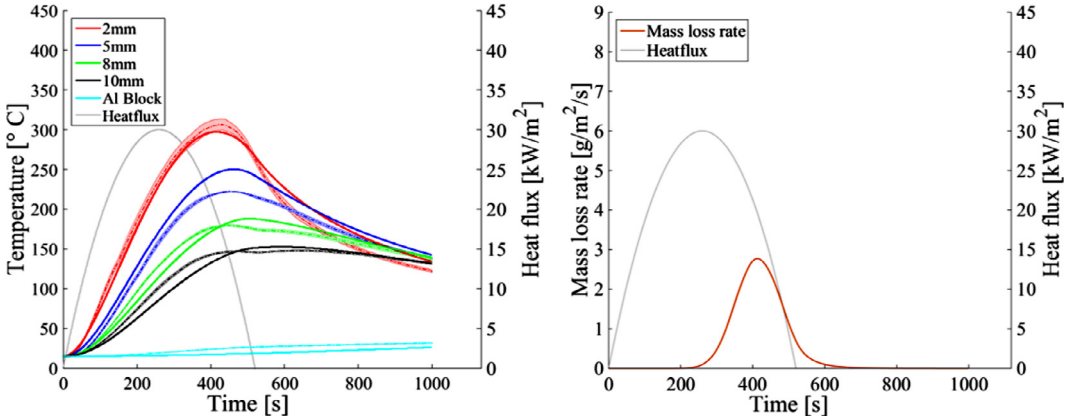

Fig. 15. Transient irradiation peaking at 30 kW/m^2 after 260 s: temperature(a) and predicted mass loss (b) response at different depths of a PMMA sample; predictions shown in solid, experiments with dashed line; error ranges are shown as clouds (sometimes too thin to see).

proportionality factor between the time and the energy-squared. However, this proportionality factor is dependent on the irradiation scenario.

The critical mass loss rate provides a wide range of critical values (from 4.1 to 9 g/m^2 s), limiting the accuracy of the criterion. As shown in Fig. 17, the samples that did not ignite show a mass loss range below the threshold value of 3 g/m^2 s. The value of 3 g/m^2 s is also found often in literature for the critical mass loss rate of PMMA ([3,15]). Therefore the concept of minimum threshold for mass loss rate is introduced here, below which ignition will not occur and a value that was not reached when samples ignited. However, the mass loss results were obtained numerically and need experimental confirmation. Overall, this threshold seems to be the most viable way of estimating whether or not ignition will occur.

Table 8
Ignition conditions as observed in experiments and predictions; ignition criteria used, in order: critical temperature, critical energy, time-energy squared, critical mass loss rate.

Experiment	t_{ig} (s)	T_{ig} (°C)	T_{max}[a] (°C)	Q_{ig} (Eq. (2)) (MJ/m^2)	Q_{total}[b] (MJ/m^2)	C (Eq. (3)) (GJ^2/m^4 s)	$\dot{m}''_{ig}$ (g/m^2 s)	$\dot{m}''_{max}$[a] (g/m^2 s)
15 kW/m^2 constant	–	–	330	–	60	–	–	2.5
20 kW/m^2 constant	520	320	–	11.2	–	240	4.9	–
30 kW/m^2 at 320 s	450	360	–	10.0	–	222	5.2	–
45 kW/m^2 at 320 s	300	383	–	8.8	–	258	9.0	–
25 kW/m^2 at 320 s	–	–	290	–	10.7	–	–	1.7
30 kW/m^2 at 480 s	475	335	–	9.4	–	186	4.1	–
30 kW/m^2 at 260 s	–	–	306	–	10.4	–	–	2.8
Literature	–	380 [4]	–	2 [5]	–	226 [6]	3.0 [11]	–

[a] T_{max} and $\dot{m}''_{max}$ when ignition did not occur.
[b] $Q_{total} = \int_0^{t_{end}} \dot{q}''_e dt$, where t_{end} is the time to the end of experiment where ignition did not occur.

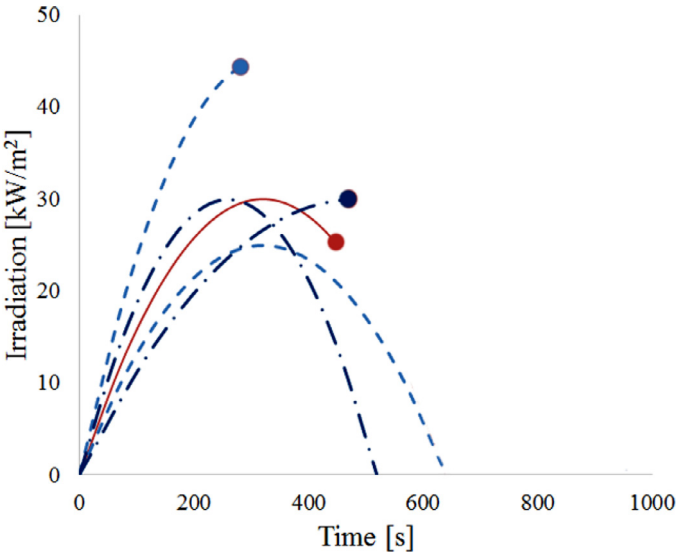

Fig. 16. Overview of experimental measurements of the time to ignition for all transient irradiation pulses. The ones where ignition occurred, the irradiation pulse is shown only until ignition time.

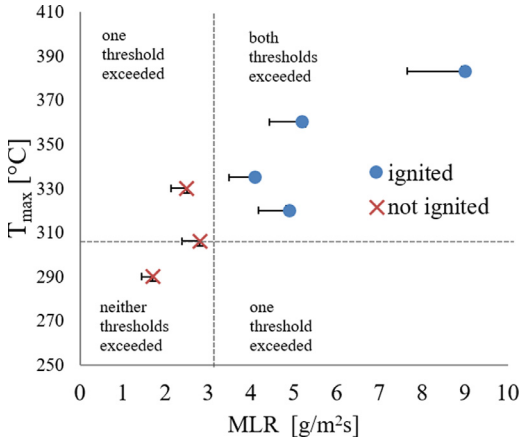

Fig. 17. Minimum threshold values for mass loss rate and temperature; the lower left part of the plot shows the area where ignition will not occur (i.e. under a mass loss rate of 3 g/m^2 s and a temperature of 305 °C) and the upper right part represents the area where ignition will occur.

The next criterion is the critical temperature. This criterion has shown a capability of estimating a range of temperatures at which PMMA will ignite, with an average of 350 °C. The range of critical temperatures is wide (from 320 to 384 °C) and the criteria provides a

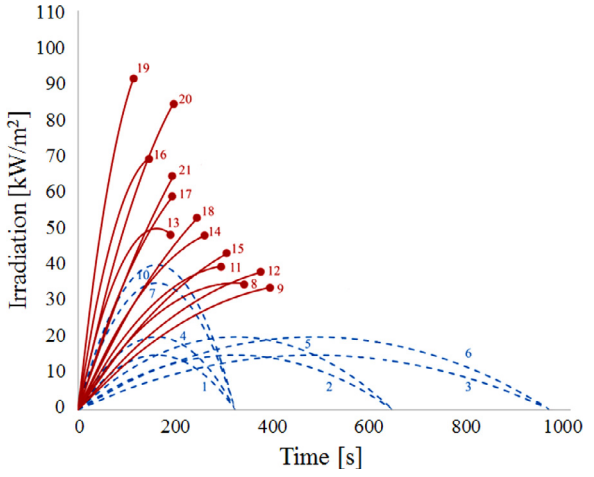

Fig. 18. Predicted time to ignition of different parabolic heat fluxes using a critical mass loss rate of 3 g/m^2 s.

range of times to ignition. Nevertheless, similar to the mass loss rate, our data shows a minimum threshold value, below which ignition does not occur. Figure 17 collects all the mass loss rate and temperature information from the experiments and predictions in this work. Observing the results, the threshold value for temperature is 305 °C. The value at 330 °C is considered an outlayer and comes from an experiment under constant irradiation.

This analysis shows that the minimum thresholds for mass loss rate and temperature offers the earliest possible time to ignition, the other criteria estimate a range of possible ignition times.

6. Predictions using the minimum threshold for mass loss rate and temperature

The model was used to predict the ignition of 21 more scenarios using the critical mass loss rate criterion. We predict in Table 8, when mass loss rate did not reach 3 g/m^2 s, the sample did that not ignite. Therefore, this value was taken as a reference for establishing whether or not ignition occurs.

The scenarios used in this application have peak irradiation ranging from 15 kW/m^2 to 100 kW/m^2. The times to peak irradiation are 160 s, 320 s and 480 s. A summary of the scenarios and their time to ignition, if it occurs, is shown in Table 9.

Table 9 also shows the good correlation between the minimum threshold for mass loss rate and the minimum threshold for surface temperature. The values of temperature when the sample reaches a mass loss rate of 3 g/m^2 s fall mostly in the range of 300–305 °C. Based on the ignition experimental results presented in Table 8 as well as the modelling application, a value of 305 °C is confirmed to

Table 9
Ignition predictions using the model and a critical mass loss value of 3 g/m^2 s.

Scenario	Peak irradiation (kW/m^2)	Time to peak (s)	Time to ignition (s)	Surface temperature at ignition (°C)
1	15	160	–	–
2	15	320	–	–
3	15	480	–	–
4	20	160	–	–
5	20	320	–	–
6	20	480	–	
7	35	160	–	–
8	35	320	331	300
9	35	480	395	300
10	40	160	–	–
11	40	320	294	301
12	40	480	355	300
13	50	160	186	305
14	50	320	245	303
15	50	480	300	302
16	70	160	307	
17	70	320	193	306
18	70	480	238	304
19	100	160	110	313
20	100	320	189	361
21	100	480	190	308

serve as a threshold. These modelling results confirm that when both minimum thresholds are exceeded, ignition takes place some time afterwards, whereas if neither threshold are exceeded, ignition will not occur at any time. This provides a conservative approach to establish the earliest possible time to ignition.

Figure 18 summarises the results of the simulations presented in Table 9. When exposed to a low irradiation of 15 or 20 kW/m^2, the sample is predicted to not ignite, regardless of the heating rate, because the mass loss rate never reaches 3 g/m^2 s. The same is valid when 35 or 40 kW/m^2 is reached at 160 s, when the sample does not ignite because the exposure to the irradiation is not long enough. In all the other scenarios, the model predicts that the sample will ignite. The results of the predicted times to ignition show that the at high heat fluxes (over 50 kW/m^2), the samples will ignite faster when the time to peak is shorter. When the irradiation is lower, such a short time to peak does not produce a high enough mass loss rate to cause ignition.

7. Conclusion

We have used transient irradiation to study the process of pyrolysis and ignition of PMMA samples by combining computational and experimental approaches.

Heating a fuel sample with transient irradiation is a much more realistic fire scenario than a constant source. Moreover, transient irradiation is the comprehensive scenario for fire research and the general case for solid ignition. Apart from the present work, all but two studies in the fire science literature consider constant irradiation.

We have investigated transient irradiation with parabolic pulses (simplest curve including both growth and decay) which for the base case is at 30 kW/m^2 after 320 s. The base case is then altered to investigate the influence of increasing and decreasing the peak heat flux (45 and 25 kW/m^2) and the time to peak (480 and 320 s). The model, based on heat transfer, single step chemistry and temperature dependent properties, was validated first against benchmark experimental data [9] under constant irradiation. The comparison with the transient irradiation shows good agreements with the measured in-depth temperature profiles with an average error below 9%.

Model and experiments are combined to study the validity of the different ignition criteria found in the literature. We find that of these criteria, the best predictions are provided by the critical mass loss rate followed by the critical temperature, and the worst is the critical energy.

Further analysis reveals the novel concept of simultaneous minimum threshold values. While the mass loss rate is below 3 g/m^2 and the surface temperature is below 305 °C, ignition does not occur. Therefore these threshold values when exceeded simultaneously establish the earliest time possible for ignition.

Acknowledgments

The authors thank FM Global for funding this work. Also, the support of Juan Hidalgo-Medina in assisting with the experimental set-up and the fruitful discussions with Xinyan Huang and Francesco Restuccia are gratefully acknowledged.

References

[1] H.C. Hottel, Stimulation of fire research in the United States after 1940, Combust. Sci. Technol. 39 (1984) 1–10.
[2] C. Fernandez-Pello, On fire ignition, Fire Safety Science—Proceedings of the Tenth International Symposium, Internatonal Association for Fire Safety Science (2011) 25–42.
[3] D. Drysdale, An introduction to fire dynamics, John Wiley and Sons, 2011, pp. 225–275.
[4] J.L. Torero, Flaming ignition of solids fuels, in: SFPE Handbook of Fire Protection Engineering, 4th ed., National Fire Protection Association, 2008, pp. 2-260–2-277.
[5] V. Babrauskas, Ignition Handbook, Fire Science Publishers, 2003, pp. 234–251.
[6] P. Reszka, P. Borowiec, T. Steinhaus, J.L. Torero, A methodology for the estimation of ignition delay times in forest fire modelling, Combust. Flame 159 (12) (2012) 3652–3657.
[7] C. Belcher, R. Hadden, G. Rein, J. Morgan, N. Artemieva, T. Goldin, An experimental assessment of the ignition of forest fuels by the thermal pulse generated by the cretaceous-paleogene impact at chicxulub, J. Geol. Soc. 172 (2) (2015) 175–185.
[8] C. Lautenberger, C. Fernandez-Pello, Generalized pyrolysis model for combustible solids, Fire Saf. J. 44 (6) (2009) 819–839.
[9] T. Kashiwagi, T.J. Ohlemiller, A study of oxygen effects on nonflaming transient gasification of PMMA and PE during thermal irradiation, Symp. (Int.) Combust. 19 (1) (1982) 815–823.
[10] N. Bal, G. Rein, Numerical investigation of the ignition delay time of a translucent solid at high radiant heat fluxes, Combust. Flame 158 (6) (2011) 1109–1116.
[11] D. Rich, C. Lautenberger, J.L. Torero, J. Quintiere, C. Fernandez-Pello, Mass flux of combustible solids at piloted ignition, Proc. Combust. Inst. 31 (2) (2007) 2653–2660.
[12] D.B. Spalding, Some Fundamentals of Combustion, Butterworths, London, 1955.
[13] D. Drysdale, H.E. Thomson, Critical mass flowrate at the firepoint of plastics, Fire Saf. Sci. 2 (1989) 67–76.
[14] R. Lyon, J. Quintiere, Criteria for piloted ignition of combustible solids, Combust. Flame 151 (2007) 551–559.
[15] N. Bal, Uncertainty and complexity in pyrolysis modelling, (Ph.D. thesis), The University of Edinburgh, 2012.
[16] ASTM Standard E2058, Standard test methods for measurement of material flammability using a fire propagation apparatus (FPA), Technical Report, West Conshohocken, PA, 2013.
[17] P. Reszka, J.L. Torero, In-depth temperature measurements in wood exposed to intense radiant energy, Exp. Therm. Fluid Sci. 32 (7) (2008) 1405–1411.
[18] R. Carvel, T. Steinhaus, G. Rein, J. Torero, Determination of the flammability properties of polymeric materials: A novel method, Polym. Degrad. Stab. 96 (2011) 314–319.
[19] C. Lautenberger, Gpyro: a generalized pyrolysis model for combustible solids technical reference, Technical Report, Department of Mechanical Engineering, University of California, Berkeley, Berkeley, 2009.
[20] N. Bal, G. Rein, Relevant model complexity for non-charring polymer pyrolysis, Fire Saf. J. 61 (2013) 36–44.
[21] N. Bal, J. Raynard, G. Rein, J.L. Torero, M. Försth, P. Boulet, G. Parent, Z. Acem, G. Linteris, Experimental study of radiative heat transfer in a translucent fuel sample exposed to different spectral sources, Int. J. Heat Mass Transf. 61 (2013) 742–748.
[22] C. Lautenberger, A generalized pyrolysis model for combustible solids (Ph.D. thesis), University of California, Berkeley, 2007.
[23] European Aluminium Association, Aluminium: physical properties, characteristics and alloys, Technical Report, Banbury, UK, 1994.